Observations of Collimated Ionization Channels in Aluminum-Coated Glass Targets Irradiated by Ultraintense Laser Pulses

M. Borghesi,* A. J. Mackinnon,† A. R. Bell, G. Malka,‡ C. Vickers, and O. Willi
The Blackett Laboratory, Imperial College of Science, Technology and Medicine, London SW7 2BZ, United Kingdom

J. R. Davies
Instituto Superior tecnico, GoLP, 1096 Lisboa, Portugal

A. Pukhov§ and J. Meyer-ter-Vehn
Max-Planck-Institut für Quantenoptik, D-85748 Garching, Germany
(Received 28 December 1998)

Filamentary ionization tracks have been observed via optical probing inside Al-coated glass targets after the interaction of a picosecond 20-TW laser pulse at intensities above 10^{19} W/cm^2. The tracks, up to 700 μm in length and between 10 and 20 μm in width, originate from the focal spot region of the laser beam. Simulations performed with 3D particle-in-cell and 2D Fokker-Planck hybrid codes indicate that the observations are consistent with ionization induced in the glass target by magnetized, collimated beams of high-energy electrons produced during the laser interaction.

PACS numbers: 52.40.Nk, 52.50.Jm, 52.65.–y, 52.70.Kz

Recent computational papers have predicted that, during the interaction of ultraintense laser pulses with dense plasmas, collimated beams of very energetic electrons are produced [1–3]. In particular, particle-in-cell (PIC) simulations predict that MeV electrons, ponderomotively accelerated along the propagation axis, are radially confined by large, self-generated magnetic fields [2]. This can lead to a well collimated electron beam propagating into the target [4]. Recent experimental results seem to indicate that the electron beam stays collimated during its propagation through a solid plastic target [5]. This was inferred from observations of small extent plasma plumes on the rear of 200 μm thick CH targets irradiated at an intensity of 10^{19} W/cm^2. Simulations performed with a Fokker-Planck hybrid code [6] suggest that inside the solid target the electrons are collimated by a magnetic field generated at the edge of the electron beam. The production and propagation of electron beams through high density plasmas are of topical interest for fast ignitor applications [7]. It is essential for this scheme to be successful that the electron energy required to start ignition is deposited in the high density core of the compressed fusion fuel. These electrons are produced at densities close to critical and have to propagate to the core through a high density plasma. So far no direct observations of collimated electron beams have been reported.

This Letter reports on experimental observations of the interaction of ultraintense laser pulses with aluminum-overcoated solid glass (SiO_2) targets. Time-resolved optical probing revealed, immediately after the interaction, the presence of narrow opaque filaments in the glass. Computational modeling indicates that the observations are consistent with collimated propagation of a fast electron beam through the target.

The experiment was performed at the Rutherford Appleton Laboratory using the Vulcan Nd:glass laser operating in the chirped pulse amplification (CPA) mode [8]. The targets were glass microscope slides, 250–300 μm wide and about 2 cm long. One of the narrow sides of the target was overcoated with a 1–3 μm thick aluminum layer to prevent direct laser transmission (see Fig. 1). The 1.054 μm CPA interaction pulse, 1 ps in duration, with an energy of about 20 J was focused by an $f/4.5$ off-axis parabola at normal incidence onto the center of the coated side of the target. The focal spot was between 8 and 10 μm in diameter at full width at half maximum (FWHM), containing 30%–40% of the energy on target giving mean intensities up to 2×10^{19} W/cm^2. A fraction of the CPA pulse was compressed with a separate pair of gratings to a duration $\tau_p = 6$ ps (FWHM), frequency doubled in a potassium dihydrogen phosphate crystal and used as a temporally independent probe. The probe, a collimated beam with a diameter of about 3 mm and an intensity in the range 10^{10}–10^{11} W/cm^2, propagated through the target along a direction transverse to the interaction axis. The relative timing between the probe and the interaction pulse was controlled within a few picoseconds. A microscope objective, with an f number of 4, imaged the target with a magnification of 55 onto photographic

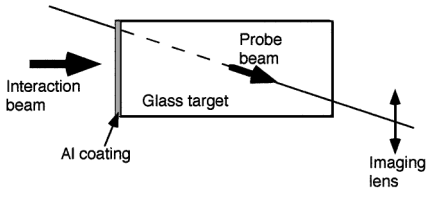

FIG. 1. Schematic of the experimental arrangement.

film resulting in a spatial resolution of 2–3 μm in the target plane.

Computational codes were used to investigate the separate issues of the electron generation and propagation in the target. The 3D PIC code VLPL [2] was used to investigate the spatial characteristics of fast electron production in an un-ionized target. The Fokker-Planck hybrid code described in Refs. [6] and [9] was used to study the propagation of the electron beam through the solid. The code represents the fast electrons with a Fokker-Planck equation, including collisional drag and random angular scattering, which is solved using a particle, Monte Carlo method. The background electrons are represented by $\mathbf{E} = \eta \mathbf{J}_b$, where η is the resistivity and $\mathbf{J}_b$ the background current density. Rotational symmetry is assumed, and the fields are found by solving Maxwell's equations, neglecting the displacement current.

Shadowgrams of the target were collected at different times. Before the interaction beam is focused onto the target, the glass slides are transparent to the probe radiation. Immediately after the interaction, tracks opaque to the probe extending into the target were observed. A typical image is shown in Fig. 2. The image has been taken with the probe nominally coincident with the interaction, i.e., integrated between $-\tau_p/2$ and $+\tau_p/2$. The target is mostly still transparent to the probe light, although it is becoming opaque near the interaction region (in the inner target region nonuniformities in the probe illumination affect the homogeneity of the image background). In particular, a track, with a 10 μm radius, can be observed originating from the interaction region and extending into the target for 300–350 μm. Similar tracks were also observed on targets with a 3 μm aluminum overcoat. Also, on some of the images more than one track can be seen; in these cases the tracks, separated by a distance of the order of 10 μm, are parallel or slightly diverging ($\sim f/10$). Typical lengths of the tracks at this timing are in the range 300 to 500 μm. In images recorded at a nominal time of +3 ps (i.e., integrated up to 5–6 ps), the tracks extend up to 600–700 μm. The tracks have a roughly constant transverse size along their length, typically of the order of 10–20 μm. At about 5–8 ps after the interaction, the part of target in the field of view of the imaging system (about 1.5 mm in length) became completely opaque to the probe, limiting our experimental observations to the temporal range 0–5 ps. A similar phenomenon has been observed at lower irradiances and attributed to the propagation of a radiative ionization front into the target [10].

The opaque regions in the field of view of the probe correspond to regions in which a dense plasma is present. Under these conditions, the probe does not propagate through the plasma due to the combined effects of absorption in the plasma, reflection at the critical density and refraction due to the density gradients. It is therefore reasonable to infer that the opaque tracks correspond to localized, ionized regions inside the target. The possibility that this localized ionization is due to the propagation through the solid of a collimated beam of hot electrons was investigated using the PIC and Fokker-Planck hybrid codes. This assumption is based on experimental and theoretical evidence for the generation of high-energy electrons in ultraintense laser solid interactions [1–3,11], and on reported predictions of mechanisms leading to their collimation in overdense plasmas and solid targets [2–6].

The 3D PIC code (VLPL) [2], previously used to model the generation of fast electrons in laser plasma interactions, was used to model the electron generation in conditions close to the experiment, studying the interaction of a 10 TW, 700 fs, 6 μm radius laser pulse with a high density un-ionized silicon target, at an ion density of 5×10^{21} cm^{-3} (silicon being similar to aluminum and a major constituent of glass). A 3D PIC simulation using solid density and the spatial scales of the experiment is not currently possible. Barrier suppression ionization by electric fields is included in the code, while interparticle collisions and collisional ionization are not implemented. The simulation results are shown in Fig. 3. At the left edge of the target a region of full ionization, and compression due to the laser ponderomotive force, is clearly visible. Inside the target a series of ionized filaments are observed.

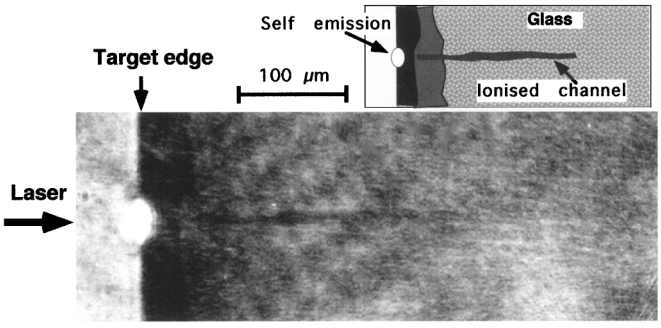

FIG. 2. Shadowgram taken during the interaction of a 20 TW, 1 ps pulse with a solid glass target coated with 1 μm of Al.

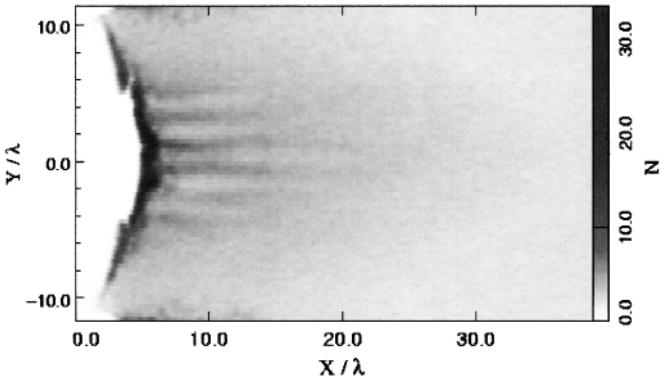

FIG. 3. PIC code simulation of the interaction of a 10 TW laser pulse with un-ionized Si (ion density of 5×10^{21} cm^{-3}). The plot shows a 2D on-axis cut of the electron density ($N = n/n_{cr}$) at the time of the laser pulse peak.

These structures correspond to a current of fast electrons which splits into filaments due to the Weibel instability [2]. The electrons have a Boltzmann-like energy spectrum with an effective temperature of $KT_f = 1.5$ MeV. As the code does not include collisions, the ionization is due to collective electric fields produced by the electron jets. When the electron jets propagate through a non-ionized medium, they create fields due to the associated space charge. Also, the magnetic fields rising in time as the jets propagate induce electric fields due to Faraday's law. Near the interaction region and at the peak of the pulse field ionization is expected to be dominant, as the fields generated by the fast electrons are large enough to cause instant ionization of the material, while the high energy of the electrons means that over the distances considered they are almost collisionless. An ionized region of about 10 μm diameter with small scale filaments inside is observed. Each of the filaments is surrounded by a magnetic field, as observed in [2]. The electron jets are parallel to the laser axis and form a closely packed bundle of ionized filaments. This would appear as a single channel opaque to transverse optical probing, as observed in the experiment.

The Fokker-Planck hybrid code was used to model the propagation of an electron beam through a solid SiO_2 target. The setup used was very similar to that in [6] using the procedure given in [9]. Collision coefficients for solid SiO_2 [9,12] were used. The resistivity was $\eta = 1/(1/\eta_0 + 1/\eta_{\text{Spitzer}})$ [6], with the initial, maximum resistivity $\eta_0 = 2 \times 10^{-6}\ \Omega$ m, in agreement with experimental results [13], and $Z \ln\Lambda = 20$ in the Spitzer resistivity with the temperature given by the heating of the target. The specific heat capacity was taken from a simple fit to the results of the Thomas-Fermi model. The fast electron generation was modeled using the following parameters: peak laser intensity 2×10^{19} W/cm^2, spot radius 6 μm, pulse length 1 ps, giving a laser energy of about 20 J, fast electron temperature given by $KT_f = 1.4(I_{19})^{1/2}$ MeV, where I_{19} is the intensity in units of 10^{19} W cm^{-2}. This relation was chosen as for $I_{19} > 1$ it gives KT_f approximately equal to the maximum oscillation energy of an electron in the laser electric field, as consistent with PIC results reported here and previously [1]. The conversion into fast electrons was 30%, consistent with reported experimental observations [14].

The background heating 2 ps after the peak of the pulse is shown in Fig. 4. An exact comparison with the experiment is difficult, as the code does not give the total free electron density and the experimental results will also be affected by the time integration and uncertainties in the probe timing. However, the steep temperature gradient in Fig. 4 shows quite a clear boundary, and, for example, the 1 eV profile gives a reasonably good indication of the size of the heated region (i.e., of the region ionized by the passage of the electrons). There are two strong points of comparison with the experimental results: (i) the heated region has a roughly constant diameter, and (ii) it penetrates 400–500 μm. The diameter of the heated region depends on the transverse size of the electron source, which in the code is taken to be of the order of the focal spot. The code predicts that 5 ps after the peak of the pulse the beam has penetrated up to 600 μm into the target. By this time the electrons have lost 78% of their energy and the heat front penetration has largely stopped. These comparisons also apply to the individual tracks in the case where multiple tracks were seen. The multiple filaments detected in some experimental observations showed no sign of interacting with each other, moving straight into the target. This is also consistent with the code results where the magnetic field falls rapidly outside the beam. This is due to the fact that the total return current balances the total fast electron current, and the magnetic field (with a maximum value of 9 MG) arises as the return current is spread over a slightly larger radius. The magnetic field is not sufficient to pinch the electron current, leaving the radius of the beam roughly constant. This is because Ohmic heating leads to lower electric fields in regions of higher fast electron current densities, and consequently to a lower magnetic field. This prevents pinching, as discussed in [6], and would also tend to prevent other magnetic field driven instabilities such as the kink instability. To check that the agreement with the data is not an artifact of the specific setup used some of the code parameters were varied. Varying the cone angle between 0° and 35°, the absorption between 20% and 40% and halving the resistivity made little difference to the overall results. Increasing η_0 above $2 \times 10^{-6}\ \Omega$ m led to an increase in the width of the heated region, which was greater nearer the fast electron source, due to the increased radial diffusion of the background current which causes Ohmic heating. For values of η_0 greater than 2.5×10^{-6}, this effect led to significant lateral transport behind the target surface as described in [6]. Using a fast electron temperature $KT_f = 0.46(I_{19})^{1/3}$ MeV, as determined experimentally in [15] and used in previous simulations [6], reduced the penetration depth to about 300 μm, the propagation ceasing 3 ps after the peak of the pulse. This does not agree with

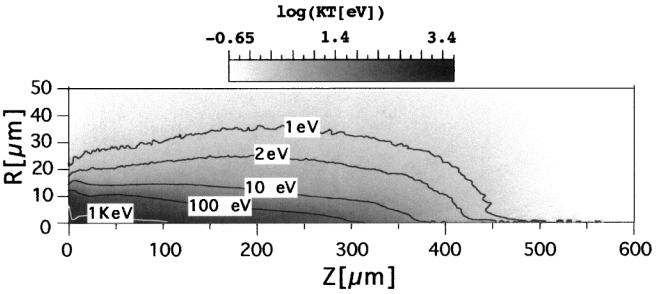

FIG. 4. Profile of background heating in eV as predicted by the hybrid code at 2 ps after the peak of the pulse.

the experimental observations. The simulations appear to confirm the hypothesis that the ionization tracks observed in the experiment are due to magnetically collimated fast electrons. Among other possible causes, ionization due to direct laser propagation is highly unlikely due to the presence of the Al coating that makes the front of the target opaque to the laser radiation. Because of the effect of the prepulse and the rising edge of the pulse, the main part of the pulse will interact with a short scale length plasma, with a profile rising from underdense to highly overdense values. Ionization due to propagation of high harmonics of the laser wavelength seems also unlikely, as, in order to propagate through the solid density plasma ahead of the interaction region, the harmonics should be in the extreme ultraviolet (XUV) region, and glass is opaque to radiation in this range of wavelength. However, XUV light could propagate through a region preheated by the fast electrons, and therefore contribute to some extent to the observed experimental features.

Some information about the fast electron and target parameters can be drawn from the comparison of the experimental and computational results. The dependence of the penetration depth on fast electron temperature indicates that KT_f is of the order of a MeV, in disagreement with the experimentally determined scaling $KT_f = 0.46(I_{19})^{1/3}$ MeV, obtained at lower intensities [15], but in agreement with PIC codes [1,2] and recent experimental results [11]. This may indicate a transition in the mechanism of fast electron generation from resonance absorption to direct ponderomotive acceleration. The code results for penetration depth are at the lower end of the range observed in the experiment. The most likely reason for this appears to be that the actual fast electron temperature was higher, due to a laser irradiance higher than the nominal one. This could be due to better focusing achieved in some shots, or to the fact that the pulse could undergo some relativistic self-focusing in the preplasma present in front of the target, leading to a higher intensity than in vacuum. Indeed, relativistic self-focusing has been observed in 2D PIC simulations of an ultraintense laser pulse propagating in an underdense plasma with a longitudinal size of a few microns and a steep density gradient [16]. As a matter of fact, in the experiment reported here the power of the laser is such to be above the critical power for relativistic self-focusing at densities larger than $0.01n_c$. The observations in which more than one filament was seen are probably also due to shot-to-shot variations of the spatial distribution of the laser intensity influencing the electron source. In addition, the sensitivity of the width of the heated region to the maximum resistivity puts an upper limit on the resistivity of the solid density plasma of about $2 \times 10^{-6}\ \Omega\,\mathrm{m}$, in agreement with previous estimates [13].

In conclusion, ionization filaments have been observed in glass targets using optical probing techniques, following laser irradiation at intensities above $10^{19}\ \mathrm{W/cm^2}$. An Al coating prevented direct laser light propagation into the target. The filaments extended several hundred microns from the target surface and maintained a roughly constant diameter of $10-20\ \mu$m along this distance. Computer modeling, performed with a 2D PIC code and a Fokker-Planck hybrid code, indicated that the observed tracks are consistent with ionization induced by magnetically collimated fast electrons. These observations are consistent with hypotheses drawn on previous experimental results and provide an important insight into the physics of the propagation of electron beams in solids and dense plasmas, a subject of topical interest in view of applications such as the fast ignitor. This result also allows estimates of the fast electron temperature and the resistivity of the solid density plasma formed by the fast electrons.

The authors acknowledge the help of the staff of the Central Laser Facility. This work was funded by ESPRC/MoD grants and a TMR Marie Curie Research Fellowship.

*Present address: Department of Pure and Applied Physics, The Queen's University of Belfast, Belfast BT7 1NN, UK.
†Present address: Lawrence Livermore National Laboratory, Livermore, CA.
‡Present address: Centre d'Etudes Nucleaires de Bordeaux Gradignan, Domaine du Haut-Vigneau, BP 120, Université de Bordeaux 1, 33175 Gradignan Cedex, France.
§On leave from Moscow Institute for Physics and Technology, Dolgoprudny, 141700 Russia.

[1] S.C. Wilks *et al.*, Phys. Rev. Lett. **69**, 1383 (1992); S. Wilks, Phys. Fluids B **5**, 2603 (1993).
[2] A. Pukhov and J. Meyer-ter-Vehn, Phys. Rev. Lett. **79**, 2686 (1997).
[3] R.J. Mason and M. Tabak, Phys. Rev. Lett. **80**, 524 (1998).
[4] H. Ruhl *et al.*, Phys. Rev. Lett. **82**, 2095 (1999).
[5] M. Tatarakis *et al.*, Phys. Rev. Lett. **81**, 999 (1998).
[6] J. Davies, A.R. Bell, and M. Tatarakis, Phys. Rev. E **59**, 6032 (1999).
[7] M. Tabak *et al.*, Phys. Plasmas **1**, 1626 (1994).
[8] C.N. Danson *et al.*, J. Mod. Opt. **45**, 1653 (1998).
[9] J.R. Davies *et al.*, Phys. Rev. E **56**, 7193 (1997).
[10] T. Ditmire *et al.*, Phys. Rev. Lett. **77**, 498 (1996).
[11] G. Malka and J.L. Miquel, Phys. Rev. Lett. **77**, 75 (1996).
[12] International Committee on Radiations Units Report N.37 (I.C.R.U.), 1984.
[13] B.T. Vu, O.L. Landen, and A. Szoke, Phys. Plasmas **2**, 476 (1995); H.M. Milchberg *et al.*, Phys. Rev. Lett. **61**, 2634 (1988); A. Saemann and K. Eidmann, in *Superstrong Fields in Plasmas*, edited by M. Lontano *et al.* (AIP, New York, 1998).
[14] M.H. Key *et al.*, Phys. Plasmas **5**, 1966 (1998).
[15] F. Bet *et al.*, Phys. Plasmas **4**, 447 (1996).
[16] B.F. Lasinski *et al.*, Phys. Plasmas **6**, 2041 (1999).